

Enhancement of crack propagation resistance in epoxy resins by introducing poly(dimethylsiloxane) particles

L. REY, N. POISSON, A. MAAZOUZ, H. SAUTEREAU*

Laboratoire des Matériaux Macromoléculaires UMR CNRS No. 5627, Institut National des Sciences Appliquées, 20, avenue Albert Einstein 69621 Villeurbanne Cedex, France
E-mail: hsaut@insa.insa-lyon.fr

The physical and mechanical properties of polyepoxy DGEBA/DDA/Diuron networks toughened with Poly(dimethylsiloxane) particles have been studied. Blends have been realized with two kinds of dispersion tools: a high-speed stirrer and a twin-screw extruder. The dispersion state quality is discussed using transmission spectroscopy image analysis. Poly(dimethylsiloxane) suspension in an epoxy prepolymer was used as a toughening agent. Different particle quantities were introduced: 4, 8, 15% by weight. Static mechanical tests were performed in tension and compression on these poly(dimethylsiloxane) modified materials. A slight decrease of Young's modulus and an increase in plastic deformation capacity were noticed as the volume fraction of the modifier increased. Using linear elastic fracture mechanics (LEFM), an improvement in the fracture properties (K_{IC} , G_{IC}) was shown. Fatigue crack growth propagation studied for the blends demonstrated that the Paris law can be used to describe the behavior of the materials. Increasing the volume fraction of the modifier leads to an improvement of fatigue crack propagation resistance. Finally a decrease in the wear rate and the friction coefficient with the increase of particle quantities has been shown (in a pin on disk configuration). Toughening mechanisms are discussed with SEM fracture surfaces. © 1999 Kluwer Academic Publishers

1. Introduction

Epoxy resins are widely used as a matrix for high strength composite materials because of their high performance. Nevertheless, because these networks are highly crosslinked, they have poor crack propagation resistance.

Various ways of toughening epoxy thermosets have already been investigated. The usual way consists of the addition of rubbers or thermoplastics which are initially miscible in the epoxy system and display a phase separation during curing [1, 2]. Thus the final morphology of the dispersed phase is strongly dependent on curing conditions [3, 4]. CTBN and ATBN have been employed with great success but with appreciable loss of thermo-mechanical properties due to their miscibility with epoxy resins [2, 4, 5]. What is more, these elastomers have a relatively high glass transition temperature which limits their low temperature flexibility. Their highly unsaturated structure makes them unsuitable for use at elevated temperatures.

A new approach is now being investigated, it consists of the dispersion of preformed particles into the initial reactive systems [6–12]. Several problems arise from the addition of preformed particles. Their size and

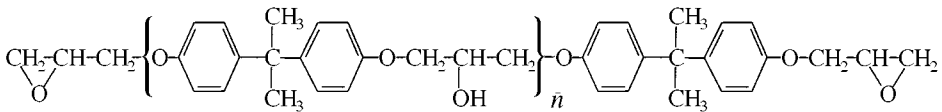
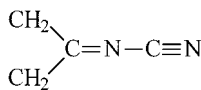
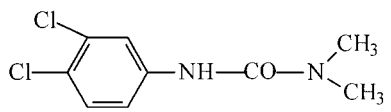
composition have to be controlled [13, 14] and surface treatments are often needed [14–17]. Moreover the introduction of particles strongly increases the viscosity of the system, which may be a drawback for processing. Last but not least, the quality of dispersion must be as good as possible to obtain toughness improvement.

In this context, silicone rubber, especially poly(dimethylsiloxane), PDMS, has a number of attractive properties: low surface tension and surface energy; extremely low glass transition temperature (about -120°C) due to high chain flexibility and low intermolecular forces; hydrophobic behavior; low solubility parameter. This last property makes PDMS immiscible with practically all thermosetting resins even before the crosslinking reaction. What is more, PDMS shows UV insensitivity, oxygen and high temperature stability [6].

This combination of excellent features makes PDMS very promising. In this present paper, we try to evaluate the enhancement of crack propagation resistance of epoxy networks with the introduction of poly(dimethylsiloxane). The integrity of mechanical and thermal properties will also be verified. Finally, a

* Author to whom all correspondence should be addressed.

TABLE I Chemical products used in synthesis of materials

Name	Chemical formula	Supplier
DGEBA	 $M\bar{n} = 382 \text{ g/mol}$ $\bar{n} = 0.15$	LY 556 CIBA GEIGY
DDA or Dicy	 <p>Dicyanamide min 97% H₂O max 3% Si max 1.6% T_f 210 °C Diameter (98% < 10 μm)</p>	DYHARD 100S SKW TROTSBERG
Diuron	 <p>M = 233 g/mol T_f = 155 °C</p>	DYHARD UR200 SKW TROTSBERG

fatigue wear test in a pin on disk configuration is shown and discussed.

2. Experimental procedures

2.1. Materials

2.1.1. Matrix

The epoxy prepolymer used in this study was based on diglycidyl ether of bisphenol-A (DGEBA) and dicyandiamide (DDA) as a hardener described in Table I. Diuron was used as a catalyst (3% by weight) because the monuron usually used in this case has been prohibited due to its toxicology. An aminohydrogen-to-epoxy ratio of 0.6 has been chosen to obtain the highest glass transition possible [17].

2.1.1.1. Rubber particles. Functionalized poly(dimethylsiloxane) particles (Hanse Chemie Albidur EP2640) were used as a dispersed phase to reinforce the epoxy matrix. They were dispersed in the DGEBA prepolymer at 40% weight and their mean diameter was about 4 μm.

2.1.1.2. Blends realization. Different particle quantities (4, 8, 15% by weight) were added to the reactive mixture. The mixing was carried out using three dispersion tools: Two high-speed mechanical stirrers (Ultraturax S50-G45G et S50-G45FF) and a twin-screw extruder. Blends were cured for 2 h at 120 °C, conforming to industrial practice. During curing the mould was kept in rotation to prevent possible sedimentation of particles and DDA. The low viscosity of the blends make them suitable for prepreg impregnation. The viscosity measurements of blends as a function of shear rate at 80 °C were carried out in a Couette flow rheometer (Rheomat 115).

2.2. Mechanical testing

2.2.1. Mechanical properties

Tensile tests were carried out at a cross-head speed of 10 mm/min with ISO60 samples on which two strain gages (Vishay Micromasures) had been placed. Young's modulus and Poisson ratio were also measured. Plastic deformation aptitude was evaluated using a compression cage on parallelepiped bars (20 × 10 × 8 mm³) in order to determine the yield stress in compression (σ_y). The yield stress, σ_y, was corrected assuming constant volume hypothesis according to the following formula (ε_y: yield strain):

$$\sigma_{yc} = \sigma_y(1 - \varepsilon_y)$$

All tests were conducted with an Adamel-Lhomargy (MTS) DY25 tensile machine.

Viscoelastic spectra were obtained with a RDA II (Rheometrics) instrument. Samples were tested in torsion between -150 and 200 °C, in strain control (0.1%) with a frequency of 10 Hz. According to the literature, three relaxations were observed: The main relaxation of PDMS particles (≈ -120 °C), the secondary relaxation (β) of epoxy (≈ -65 °C) and then the main relaxation (α) of the epoxy matrix (≈ 135 °C).

Fracture toughness (critical strain energy release rate, G_{IC}), and critical stress intensity factor (K_{IC}) were measured at 25 °C according to the protocol of the European Group of Polymer Fracture [18]. Tests were carried out on a single-edge notched (razor blade tapped) three-point bending specimen. A cross head speed of 10 mm/min was used.

2.2.2. Fatigue crack propagation (FCP)

Fatigue crack propagation tests were performed at room temperature using a Zwick REL 1853 hydraulic set-up. Compact tension specimens (CT) were used with the

specifications recommended by Williams and Cawood [18]. Sinusoidal cycling at 5 Hz was carried out under load control in tension-tension mode with a load ratio F_{\min}/F_{\max} close to zero. The maximum load was chosen in order to start the test with $\Delta K = K_{\max} - K_{\min}$ close to $K_{IC}/2$.

The crack was initiated with a razor blade at room temperature and crack growth was followed with a Vishay-Micromasures CPA 1 gage placed on one face of the CT specimen, perpendicularly to the crack propagation direction.

The FCP rates, da/dN , were determined manually as the gradients of the curves of crack growth Δa , as a function of the number of cycles, N . The related stress intensity factor range, ΔK , was calculated according the following formula,

$$\Delta K = \frac{\Delta P}{BW^{1/2}} \left(\frac{2+A}{(1-A)^{3/2}} \right) (0.886 + 4.64A - 13.32A^2 + 14.72A^3 - 5.6A^4)$$

where ΔP is the variation of the load for each cycle, B , the sample thickness, W , the width, and a , the initial crack length.

$$A = a/W.$$

2.2.3. Wear tests

The pin on disk configuration for the wear tests was a chromium steel ball (5 mm diameter) sliding on the surface of the modified epoxy slab which was exposed to air during the test. The test conditions were, normal load 14.12 N, sliding velocity 50 tr/min (17 mm diameter). The humidity and temperature could not be controlled precisely. Specimens were cleaned just before the test using acetone.

During the test, the epoxy surface was alternatively compressed and pulled by the steel ball. The stress magnitude was calculate to be 57 MPa, less than $\sigma_y/2$.

2.2.4. Microscopy

The morphology of the PDMS particles and their ability to be dispersed well into the epoxy matrix were checked by TEM (Phillips CM120) on 70–80 nm thick specimens cutted with an ultra-microtom (LEICA).

To evaluate dispersion quality, TEM micrographs were divided into 35 equal squares. It is possible to calculate an heterogeneity factor, $100\sigma/m$ (σ : standard deviation, m : average particle number per unit area). This factor enhances with the dispersion irregularity (see [5] for more details). A good dispersion has a $100\sigma/m$ value about 20 or less.

Failure modes were observed on K_{IC} and fatigue samples with a scanning electronic microscope (Phillips XL20).

3. Results and discussion

3.1. Morphology analysis

It is readily apparent from Table II that our blends are not well dispersed. Even if several research works

TABLE II Morphology analysis and dispersion state

Dispersion tool	Vol %	\bar{D}_{\max} (μm)	$100\sigma/m$	\bar{D} (μm)
Twin-screw extruder	17	2.1	133	0.82 ± 1.22
S50-G45G	12.2	3	94	0.37 ± 0.67
S50-G45FF	6.4	2.4	193	0.52 ± 0.59
S50-G45FF	11.8	2.7	145	0.58 ± 0.85
S50-G45FF	17.8	3.4	128	0.98 ± 0.67

[19, 20] have shown that a good dispersion is more efficient for enhancing resistance in crack propagation, our blends show the advantage of being stable for all concentrations and independent of the dispersion tools employed.

3.2. Viscosity analysis

The stability of the unreacted blend was checked before any curing. The presence of a dispersed second phase in the epoxy prepolymer mixture can affect the processing conditions of the blends. Thus the viscosity dependence of the PDMS/epoxy prepolymer mixture on the shear rate was studied. No increase and decrease of the viscosity variations with the shear rate was observed (Fig. 1). Thus the dispersion structure is not further modified with the processing conditions which generally induce a significant shear stress. The pure prepolymer and all blends display good Newtonian behavior and low viscosity. A slight viscosity increase for 40 wt % PDMS modified epoxy was observed but the rheological behavior was not affected. As a consequence, all the blends are suitable for prepreg impregnation (Fig. 1).

3.3. Thermal and mechanical properties of the epoxy network with different quantities of poly(dimethylsiloxane)

Thermal and mechanical properties of modified and unmodified epoxy are summarized in Table III. According to the literature, the addition of poly(dimethylsiloxane) rubber induces a slight decrease in the glass transition temperature (T_g measured with a Mettler TA3000) and in the temperature position of the main relaxation, T_{α_e} , of pure epoxy network (α_e , associated with T_g).

A slight decrease in the rubbery modulus G' (at $T_{\alpha_e} + 50^\circ\text{C}$) is observed. This decrease has been attributed to a small amount of poly(dimethylsiloxane)

TABLE III Results of static and cyclic mechanical tests

% by weight of PDMS	0	4	8	15
T_{α_e} ($^\circ\text{C}$) (1 Hz)	141	137	136	135
G' (MPa) (200 $^\circ\text{C}$)	6.1	5.5	4.1	4.4
T_g ($^\circ\text{C}$) (DSC)	125	123	122	116
E (GPa) at 25 $^\circ\text{C}$	3.86	3.45	2.82	2.68
σ_{ycorr} (MPa) at 25 $^\circ\text{C}$	110	100	91	79
K_{IC} (MPa $\cdot\text{m}^{1/2}$) at 25 $^\circ\text{C}$	0.93	1	1.36	1.25
ΔK^a (MPa $\cdot\text{m}^{1/2}$) at 25 $^\circ\text{C}$	0.58	0.72	0.97	0.93
m at 25 $^\circ\text{C}$	16.9	9.5	8.8	7
C at 25 $^\circ\text{C}$	7.3	0.017	0.001	0.0012

^afor $da/dN = 7.5 \cdot 10^{-4}$ mm per cycle.

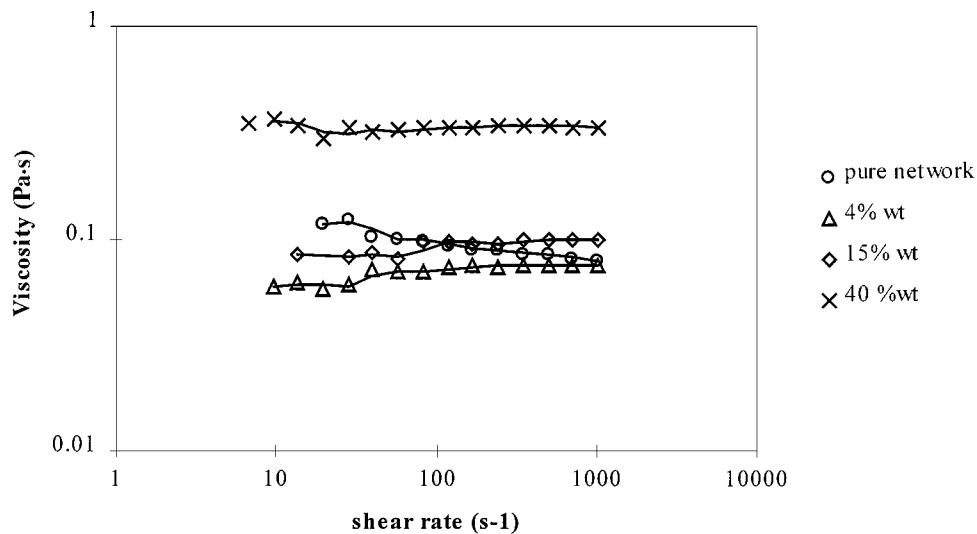


Figure 1 Variation of the viscosity with shear rate of blends at 80 °C.

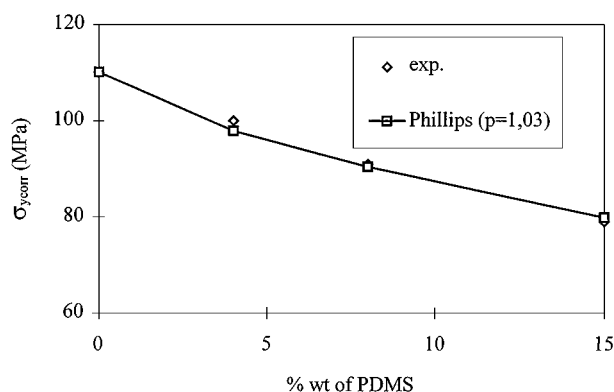


Figure 2 $\sigma_{y,corr}$ in compression test as a function of poly(dimethylsiloxane) content.

dissolved in the epoxy continuous phase [21]. This dissolved fraction has been evaluated at 7% by Fox's equation [22]. This level of miscibility is less than in the case of epoxy networks modified with ETBN8 (25% remains dissolved in the matrix in this case).

For the same reasons, Young's modulus and yield stress $\sigma_{y,corr}$ are decreasing functions of poly(dimethylsiloxane) volume fraction. Both are well described with Phillips's model [23] (with $p = 1.03$ and $\sigma_y = 3$ MPa for poly(dimethylsiloxane)). p is an adjustable parameter, for spherical particles p is $6/\pi = 1.91$ and $2/3\pi = 0.37$ for the upper and the lower bound respectively. Referring to Phillips's model [23], bonds between the epoxy matrix and the PDMS particles are not very strong (Fig. 2).

Finally, these tests show that the introduction of rubber particles increases the plastic deformation capability of epoxy networks without a dramatic loss of thermo-mechanical properties.

3.4. Fracture toughness

As we can see in Fig. 3, K_{IC} increases with the modifier content up to a threshold. This type of result is not comparable with others obtained by Block and Pyrlick [1] or Könczöl *et al.* [6] who found a maximum of

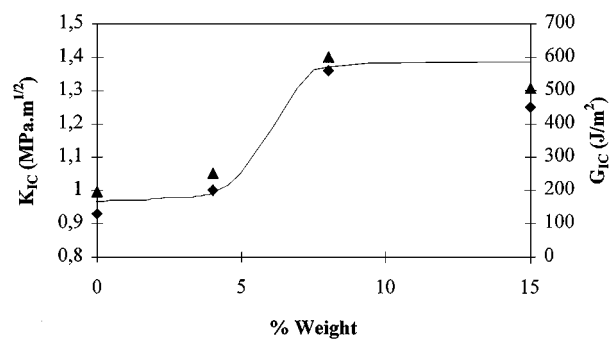


Figure 3 Dependence of the fracture toughness K_{IC} (◆) and G_{IC} (▲) of poly(dimethylsiloxane) modified epoxy networks.

reinforcement for 10% of the modifier without any consistent explanation. Yorkgitis *et al.* [21] show that this behavior depends on the poly(dimethylsiloxane) structure and particle size. Modification with pure PDMS creates big particles (50 μm) and lowers K_{IC} . If 40% of dimethyl-trifluoropropyl is included into the PDMS structure, particle size decreases (5 μm) and K_{IC} increase up to a maximum for 10% of the modifier.

Failure mode will be analyzed to try to explain this threshold of K_{IC} . Overall it can be concluded that the addition of PDMS particles in epoxy matrix improves the fracture toughness of the blend by more than 40% without a significant decrease in the T_g .

3.5. Fatigue crack propagation (FCP)

The FCP experiment plotted in Fig. 4 (in a log-log diagram) agrees well with the Paris law $da/dN = C(\Delta K)^m$ as was observed with other epoxy networks [5, 8, 9, 24].

Increasing the PDMS particle content decreases C and m up to 8% where the reinforcement stops. This result is consistent with the evolution of K_{IC} , it confirms the linear relationship between ΔK_{max} and K_{IC} (Fig. 5). This means that either in static test condition or in dynamic test condition, the failure modes are very similar.

Block and Pyrlick [1] or Könczöl *et al.* [6] found a minimum for C and m for 10% of particles added.

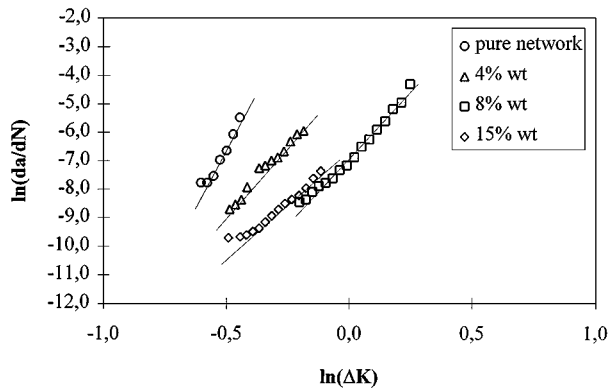


Figure 4 Paris law diagrams for crack propagation test of poly(dimethylsiloxane) modified epoxy networks.

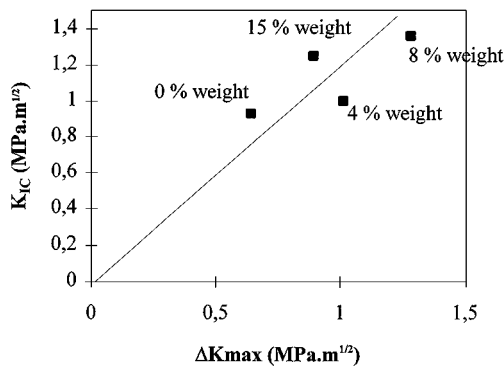


Figure 5 K_{IC} as a function of ΔK_{max} for crack propagation test of poly(dimethylsiloxane) modified epoxy networks (number indicates weight fraction of poly(dimethylsiloxane)).

These results were consistent with the evolution of K_{IC} for their materials. Several literature results are summarized in Table IV in order to compare our materials with other blends using different particles.

Becu *et al.* [5, 24] obtained better results because the dispersion of PBcoPS/PMMAcoPS/COOH core-shell particles was very good ($100\sigma/m = 20$) and their diameters were smaller (200 nm). CTBN shows good results but with a significant loss of thermal (T_g), elastic and plastic properties [2].

3.6. Failure mode

Fracture surfaces (fatigue and K_{IC}) of our materials have been observed with SEM. Pure epoxy shows a very plane fracture surface [25]. As expected, we have found

some ribs, cracks, local deviation of cracks to form river markings, all characteristics of brittle materials (Fig. 6).

When epoxy is reinforced with silicone rubber, the fracture surface becomes rough. The more slowly the crack progresses, the rougher the surface is. Karger-Kocsis and Friedrich [8] identified the mechanisms responsible for this reinforcement.

Two populations of particles have been observed. On one hand the smaller particles (diameter $0.5 \mu\text{m}$) act as stress concentrators and generate a dense network of microcracks around the main crack. On the other hand this main crack is deviated by the biggest particles (diameter $4 \mu\text{m}$), which are less bonded with matrix. No cavitation has been observed for small particles.

In fact, a non negligible part of the reinforcement is due to the small part of PDMS dissolved in the epoxy matrix. Yamini and Young [10] show that K_{IC} increases when σ_y decreases (if $\sigma_y < 110 \text{ MPa}$) because the decrease of σ_y makes the crack front smoother.

3.7. Fatigue wear test

The friction coefficient ($C_f = F_t/F_n$) as a function of the number of disk rotations for different materials is shown in Fig. 7.

After track wear was initiated by the steel ball, the friction was constant during the test. The level of friction decreases with the amount of poly(dimethylsiloxane) particles as is reported by Chitsaz-Sadeh and Eiss [11]. Yorkgitis *et al.* [21] attribute the friction coefficient reduction to a decrease in surface energy and tangential stress at the surface. Furthermore, the wear rate was evaluated by measuring the crack depth after 7000 cycles. The pure epoxy track is deeper ($24.9 \mu\text{m}$) than the 15% poly(dimethylsiloxane)/epoxy track ($13.4 \mu\text{m}$).

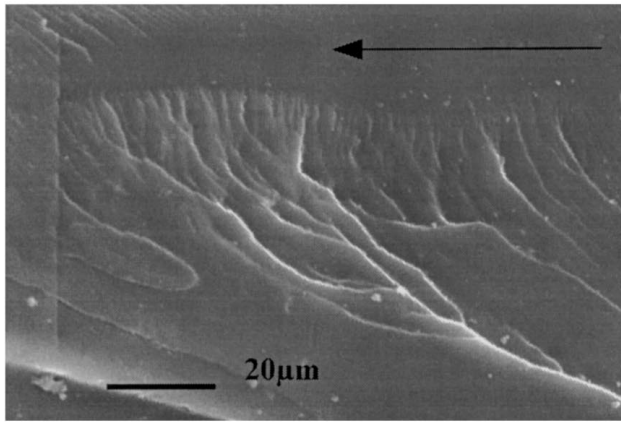
During the first rotations, the alternating stress causes cracks oriented perpendicular to the track. As the sliding continued, the cracks grow, intersect each other and sometimes generate wear particles. These particles cause extensive damage and increase the friction up to a threshold when the number of new wear particles is close to those evacuated from the track.

Not enough tests were now carried out to be able to obtain exhaustive conclusions concerning tribological phenomena that produce a decrease in friction and wear rate with the introduction of poly(dimethylsiloxane) in an epoxy matrix. But in Fig. 8 we can observe that the

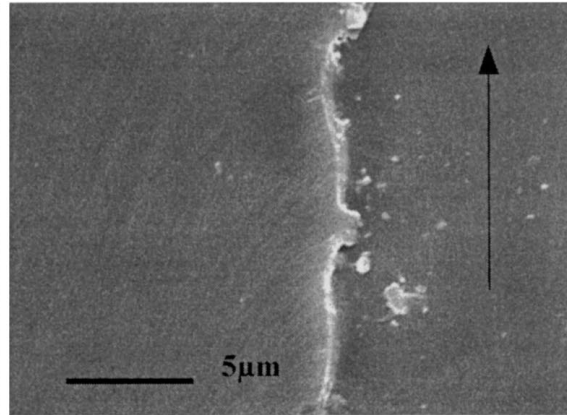
TABLE IV Comparison for fatigue tests with literature results

Ref.	Dispersed phases	wt %	C	m	ΔK_{max} (MPa · m ^{1/2})	K_{IC} (MPa · m ^{1/2})
This work	Poly(dimethyl siloxane)	0	7.3	16.9	0.64	0.93 ^a
		15	0.0012	7	0.89	1.25 ^a
Maazouz <i>et al.</i> [2]	CTBN	0	0.018	9.48	—	0.7 ^a
		15	0.0008	6.94	—	1.33 ^a
Bécu <i>et al.</i> [24]	PBcoPS/PMMAcoPS/ COOH(core-shell)	0	0.4370	8.9	0.6	0.8 ^a
		15	0.001	4.23	1.01	1.1 ^a
Karger-Kocsis and Friedrich [9]	Poly(dimethyl siloxane)	0	1000	16	0.35	1.2 ^b
		15	0.007	6.8	0.88	1.15 ^b

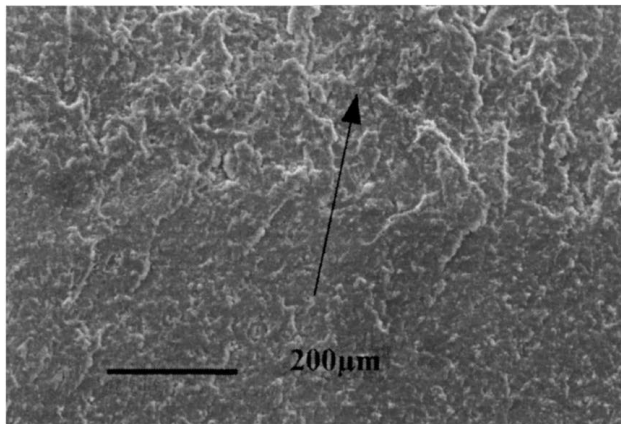
^a $v = 10 \text{ mm/min}$; ^b $v = 1 \text{ mm/min}$.



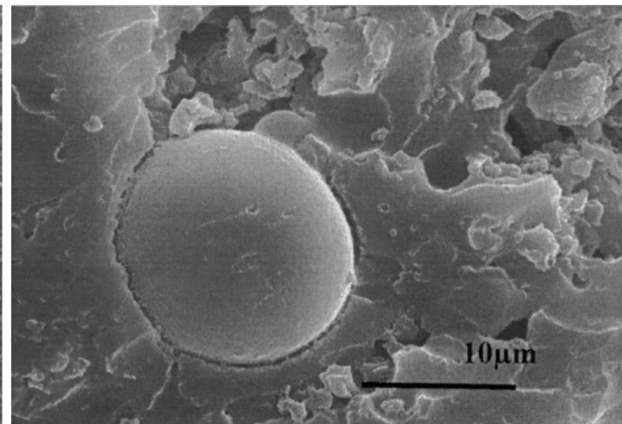
6.1



6.2



6.3



6.4

Figure 6 SEM micrographs of the static fracture surface for the pure epoxy network (6.1 and 6.2) and 15 wt % poly(dimethylsiloxane) modified epoxy network (6.3 and 6.4) (arrow indicates the crack propagation direction).

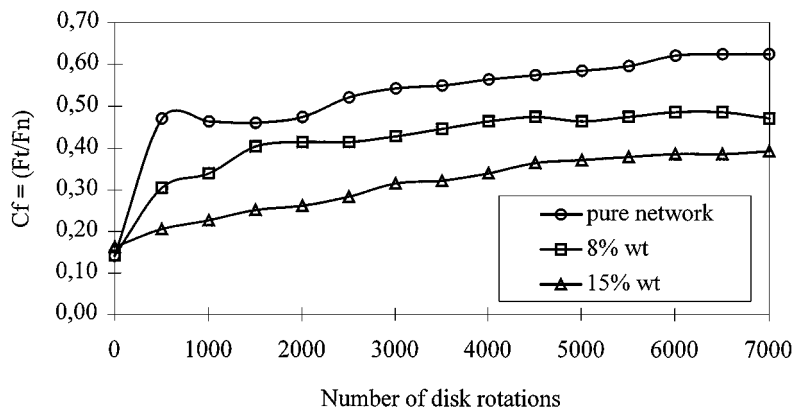


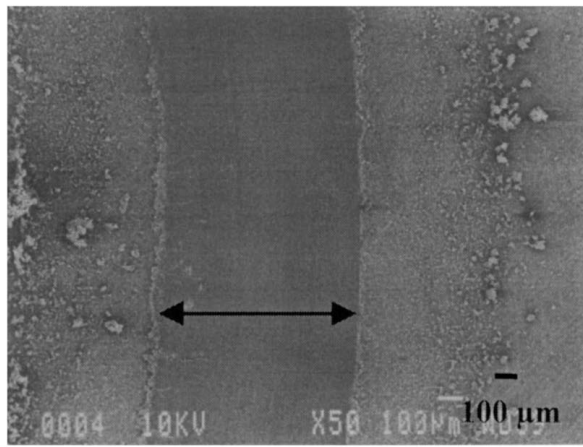
Figure 7 Friction coefficient (C_f) as a function of the disk rotations (pin on disk configuration).

epoxypoly(dimethylsiloxane) track has less wear debris than the epoxy one. Epoxypoly(dimethylsiloxane) debris seems to be less adhesive and more easily evacuated than epoxy debris. As shown in Fig. 8.2, epoxy/poly(dimethylsiloxane) debris were evacuated by the steel ball around the track in opposition with the pure epoxy track which is full of debris. It may be the reason for the difference in friction and wear rate but more investigation should be carried out to obtain a precise conclusion.

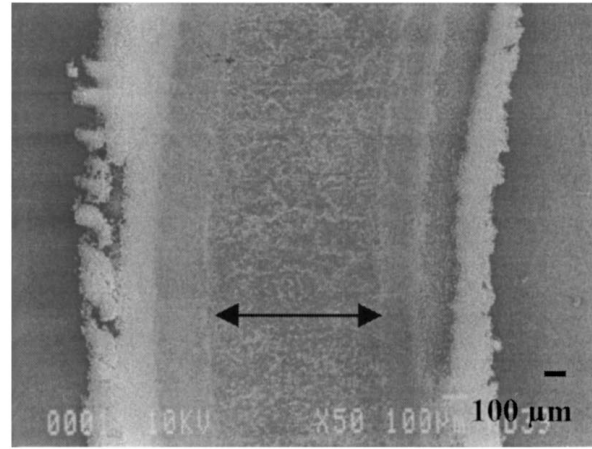
4. Conclusion

An investigation has been made to correlate morphology and the enhancement of crack propagation resistance with the introduction of PDMS particles into a brittle epoxy network. It is shown that a part of the PDMS dissolved in the matrix causes a small decrease in shear modulus and T_g and increases the plastic deformation ability.

Critical stress intensity factor (K_{IC}) and fatigue crack propagation are improved by two populations of



8.1



8.2

Figure 8 SEM micrographs of pure epoxy (8.1) and poly(dimethylsiloxane) modified epoxy networks (15 wt %) wear tracks (8.2). Arrow indicates the track width.

particles using different mechanisms well described in the literature. In both cases the resistance to crack propagation increases with the amount of particles up to a threshold (at 8% by weight).

Finally a decrease in the wear rate and friction coefficient with the introduction of PDMS was attributed to the nature of wear debris.

Work is now in progress to apply this low viscosity system to prepreg formulations and applications to structural composites.

Acknowledgement

The authors would like to thank Dr Y. BERTHIER, L. LAFARGE and M. CASSARD of the "Laboratoire de Mécanique des Contacts" of INSA de LYON (GMD-UMR 5514) for their help and advice.

References

1. H. BLOCK and M. PYRLICK, *Kunststoffe* **78** (1988) 1192.
2. A. MAAZOUZ, H. SAUTEREAU and J. F. GERARD, *Polymer Networks & Blends* **2** (1992) 65.
3. S. MONTARNAL, J. P. PASCAULT and H. SAUTEREAU, in "Rubber Toughened Plastics" Adv. Chem. Ser. No. 222, Vol. 8, edited by C. K. Riew (ACS, New Orleans, 1989).
4. D. VERCHERE, J. P. PASCAULT, H. SAUTEREAU, S. M. MOSCHIAR, C. C. RICCARDI and R. J. J. WILLIAMS, *J. Appl. Polym. Sci.* **42** (1991) 701.
5. L. BECU, H. SAUTEREAU, A. MAAZOUZ, J. F. GERARD, M. PABON and C. PICHOT, *Polym. Adv. Technol.* **6** (1994) 316.
6. L. KÖNCZOL, W. DÖLL, U. BUCHOLZ and R. MÜLHAUPT, *J. Appl. Polym. Sci.* **26** (1995) 371.
7. Y. HUANG and A. J. KINLOCH, *J. Mater. Sci.* **27** (1992) 2763.
8. J. KARGER-KOCSIS and K. FRIEDRICH, *Compos. Sci. Technol.* **48** (1993) 263.
9. *Idem.*, *Colloid Polym. Sci.* **270** (1992) 549.
10. S. YAMINI and R. J. YOUNG, *J. Mater. Sci.* **15** (1980) 1823.
11. M. R. CHITSAZ-SADEH and N. S. EISS, *Tribology Transactions* **33** (1990) 499.
12. A. MAAZOUZ, H. SAUTEREAU and J. F. GERARD, *Polym. Bull.* **33** (1994) 67.
13. H. J. SUE, E. I. GARCIA-MARTIN, D. M. PICKELMAN and P. C. YANG, in "Rubber Toughened Plastics I," Advances in Chemistry Series 233, edited by C. K. Riew (American Chemical Society, Washington, DC, 1993).
14. C. GIRODET, E. ESPUCHE, H. SAUTEREAU, B. CHABERT, R. GANGA and E. VALOT, *J. Mater. Sci.* **31** (1996) 2997.
15. F. LU, C. J. G. PLUMMER, W. J. CANTWELL and H. H. KAUSCH, *Polymer* **37** (1996) 399.
16. V. NELLIAPPAN, M. S. EL-AASSER, A. KLEIN, E. S. DANIELS, J. E. ROBERTS and R. A. PEARSON, *J. Appl. Polym. Sci.* **65** (1997) 581.
17. J. GALY, A. SABRA and J. P. PASCAULT, *Polym. Eng. Sci.* **26** (1986) 1514.
18. J. G. WILLIAMS and M. J. CAWOOD, *Polymer Testing* **9** (1990) 15.
19. D. S. KIM, K. CHO, J. K. KIM and C. E. PARK, *Polym. Eng. Sci.* **36** (1996) 755.
20. D. DOMPAS and G. GROENINCKX, *Polymer* **35** (1994) 4743.
21. E. M. YORKGITIS, C. TRAN, N. S. EISS, JR., T. Y. HU, L. YILGOR, G. L. WILKES and J. E. MCGRATH, in "Rubber-Modified Thermosets Resins," edited by C. K. Riew and J. K. Gillham (ACS No. 208, Washington, DC, 1984).
22. T. G. FOX, *Bull. Amer. Phys. Soc.* **1** (1956) 123.
23. M. G. PHILLIPS, *Compos. Sci. Technol.* **43** (1992) 95.
24. L. BECU, A. MAAZOUZ, H. SAUTEREAU and J. F. GERARD, *J. Appl. Polym. Sci.* **65**(1) (1997) 2419.
25. C. B. ARENDS, in "Polymer Toughening," edited by C. B. Arends (Marcel Dekker, New York, 1996).

Received 5 January
and accepted 20 October 1998